

The Ru^{IV}=O-catalyzed sulfoxidation: A gated mechanism where O to S linkage isomerization switches between different efficiencies

Jordi Benet-Buchholz,^a Peter Comba^{b*}, Anton Llobet^{a*}, Stephan Roeser,^a
Prabha Vadivelu^b and Sebastian Wiesner^b

a) Institute of Chemical Research of Catalonia (ICIQ)
Av. Països Catalans 16, E-43007 Tarragona, Spain

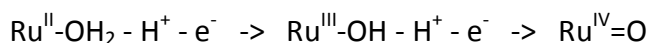
b) Universität Heidelberg, Anorganisch-Chemisches Institut,
INF 270, D-69120 Heidelberg, Germany
Fax: +49-6221-546617
e-mail: peter.comba@aci.uni-heidelberg.de

Supplementary Material

Electrochemical Analysis of $[\text{Ru}(\text{L}^2)(\text{L}^3)(\text{OH}_2)]^+$

The pH-dependent differential pulse voltammetry (DPV) of $[\text{Ru}(\text{L}^2)(\text{L}^3)(\text{OH}_2)]^+$ was performed at pH=4 ($\text{CF}_3\text{SO}_3\text{H}$) and pH=4.8 (AcOH/NaOAc , see Figure S1). According to the Nernst equation, the difference between the potentials with a pH difference of 0.8 pH units is around 47 mV; the observed difference is 40 mV, i.e. as expected within the error limit: the $\text{Ru}^{\text{III/II}}$ couple is at 0.38 V (pH=4.8) and at 0.42 V (pH=4), the $\text{Ru}^{\text{IV/III}}$ couple is at 0.72 V (pH=4.8) and 0.76 V (pH=4).

The pH dependence of the two couples is in agreement with proton-coupled electron transfer (PCET) processes, as also observed for $[\text{Ru}(\text{L}^1)(\text{OH}_2)]^{2+}$ and other similar systems,² which undergo the following processes:



The fact that $\text{Ru}^{\text{III}}-\text{OH}$ does not oxidize sulfides under the present reaction conditions is further evidence for $\text{Ru}^{\text{IV}}=\text{O}$ being the catalytically active species.

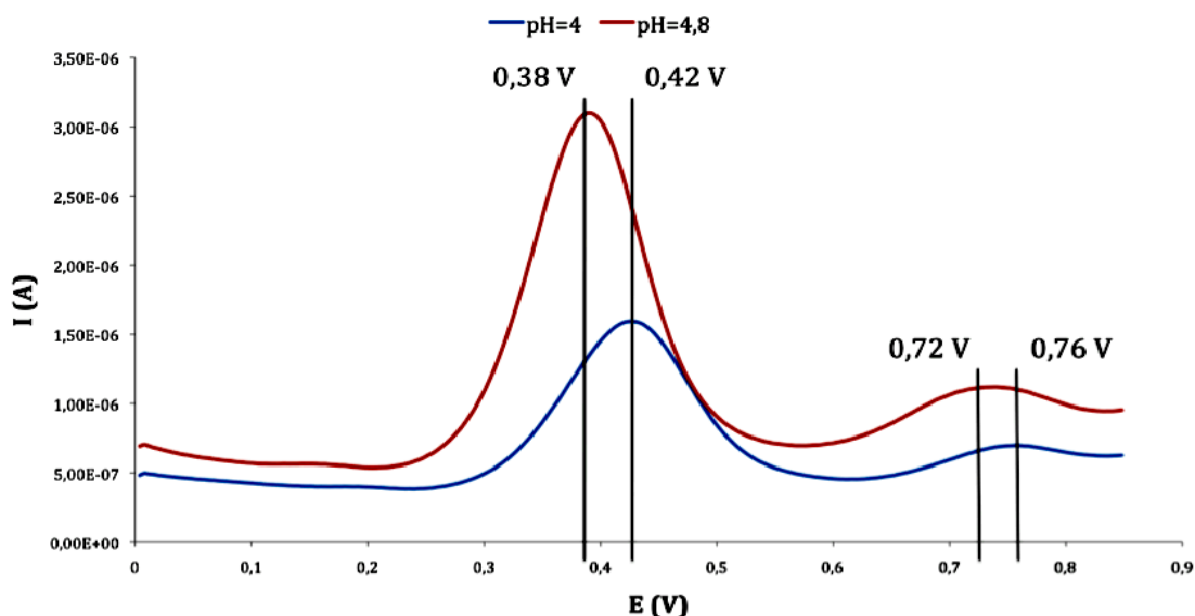


Figure S1. pH dependent differential pulse voltammogram (DPV) of $[\text{Ru}(\text{L}^2)(\text{L}^3)(\text{OH}_2)]^+$; reference electrode: SSCE, working electrode: GCWE (diameter: 3 mm), counter electrode: PtWE (diameter: 2 mm); Init E (V): 0.0; final E (V): 0.85; Incr E (V): 0.002; amplitude (V): 0.05; pulse width (sec): 0.06; sampling width (sec): 0.02; pulse period (sec): 0.2; quiet time (sec): 2; sensitivity (A/V): 10^{-6}

Computational Analysis

The interpretation that the reduced efficiency with the $[\text{Ru}(\text{L}^2)(\text{L}^3)(\text{solvent})]^+$ -based catalyst is due to an $\text{O} \rightarrow \text{S}$ linkage isomerization gate at the Ru^{II} -sulfoxide intermediate, which leads to partial inhibition in the catalytic cycle, was also probed by a DFT-based computational analysis. Unfortunately, the relative stabilities of S- and O-bonded linkage isomers of Ru^{II} -sulfoxides much depend on the functional, basis set and solvation model used and therefore are quite unreliable.^{3, 4} Although we have used a carefully optimized setup (see below), the energetics of the important linkage isomerization and solvation steps should only be interpreted on a qualitative basis. For both catalysts, the electrophilic attack of the $\text{Ru}^{\text{IV}}=\text{O}$ oxidant at the substrate sulfur atom is a very efficient process with an exceedingly low activation barrier (less than 10 kJ/mol, see Figures S2 and S3) and a large reaction free energy (approx. -100 kJ/mol).⁵ That is, the release of the relatively stable sulfoxide product (ligand exchange at the Ru^{II} -sulfoxide species) and reoxidation of the Ru^{II} precatalyst to the active $\text{Ru}^{\text{IV}}=\text{O}$ oxidant is rate limiting. The $\text{O} \rightarrow \text{S}$ linkage isomerization produces two complexes each for the ligand exchange process.

For both catalysts, as expected,^{6, 7} these are I_d processes for the O- as well as for the S-bonded forms (seven-coordinate transition states with significantly elongated Ru^{II} -thioanisoxide-O/S distances, see Figure S4). As observed experimentally with dmsO as the sulfoxide product (see Table 2 in the main text), the S-bonded form is relatively more stable for the $\text{Ru}^{\text{II}}(\text{L}^2)(\text{L}^3)$ -based than for the Ru^{II} -bispidine system (relative difference of about 35 kJ/mol). As suggested by the experiment, the deactivation of the $\text{Ru}^{\text{II}}(\text{L}^2)(\text{L}^3)$ -based catalyst is due to a significantly lower energy barrier for the linkage isomerization than in the bispidine-based system, and the barrier for the linkage isomerization in the bispidine-based system indeed is, with close to 100 kJ/mol, exceedingly high. For the $\text{Ru}^{\text{II}}(\text{L}^2)(\text{L}^3)$ -based catalyst, ligand exchange involving the more stable S-bonded sulfoxide is significantly less efficient than release of the O-bonded isomer (activation barriers of approx. 80 vs. 40 kJ/mol), while with the Ru^{II} -bispidine-based catalyst, the corresponding two activation barriers are nearly identical (70 vs. 65 kJ/mol). That is, linkage isomerization partially inhibits the catalytic cycle in the $\text{Ru}^{\text{II}}(\text{L}^2)(\text{L}^3)$ -based system, while it does not with the Ru^{II} -bispidine-based catalyst. With both catalysts, the pathway of direct release of the O-bonded isomer is more efficient than linkage isomerization (by approx. 30 kJ/mol). This is in agreement with the experimental

observations, which, even for the less efficient $\text{Ru}^{\text{II}}(\text{L}^2)(\text{L}^3)$ -based catalyst show some catalytic activity. For both systems, the linkage isomerization transition state is a seven-coordinate structure with close to identical $\text{Ru}^{\text{II}}\text{-S}$ and $\text{Ru}^{\text{II}}\text{-O}$ bond distances (see Figures S5 and S6). This is as predicted by experiment: no new signals were observed in the CV experiments when they were performed in MeCN (not shown; these are similar to those in CH_2Cl_2 reported here), i.e., MeCN does not substitute dmsO as the sixth ligand in the linkage isomerization process, and this would have been expected to occur in a dissociative reaction.

The different relative stability of the S-bonded isomer of the two catalysts must be due to differences in the electronic nature of the co-ligands and/or to steric effects. It is known that Ru^{II} complexes with predominantly σ -donor ligands prefer the S-bonded form.^{3, 8} Extra electron density on the Ru^{II} center is thought to lead to a stabilization of the Ru-S bond by π -back donation from occupied metal-d to empty sulfoxide orbitals. This is supported by the computed structures of the $[\text{Ru}(\text{L}^1)(\text{thioanisuloxide-S})]^{2+}$ and $[\text{Ru}(\text{L}^2)(\text{L}^3)(\text{thioanisuloxide-S})]^+$ complexes (see Figures S5, S6), which, for the complex with the deprotonated pyrazol-based ligand L^2 , has slightly shorter Ru-S and elongated S-O bonds (by 0.01 Å each). Steric effects in $[\text{Ru}(\text{L}^1)(\text{thioanisuloxide-S})]^{2+}$ and, more importantly, in the linkage isomerization transition state, primarily but not exclusively due to the methyl group at N3 (see above, see Figure 1 in the main text) may also lead to a destabilization of the corresponding more sterically congested structures.

All DFT calculations were carried out with the Jaguar 6.5 program package.⁹ The usual set up with B3LYP^{10, 11} and the LACVP** basis set (double ζ , with a Los Alamos effective core potential for Ru and 6-31G** for the other atoms) inverts the stability order of Ru^{II} -sulfoxides, with $\text{Ru}^{\text{II}}\text{-dmsO-O}$ more stable than $\text{Ru}^{\text{II}}\text{-dmsO-S}$ by 58 kJ/mol (L^2, L^3 complex system). This is a known problem for gas phase calculations with the B3LYP functional.^{4, 12} The SVWN functional¹³⁻¹⁵ with the LACVP** basis set well reproduces the experimentally observed trend with respect to the stability of linkage isomers. With a gas phase model the S-bonded isomer is slightly less stable than the O-bonded isomer (+2.0 kJ/mol). However, with solvation included (CH_3COCH_3 or CH_2Cl_2 , PCM)¹⁶⁻¹⁸ the S-bonded isomer is further stabilized by 10 kJ/mol. The energetic difference between the two solvents used is within a 2 kJ/mol range. Also, larger basis sets (up to LACV3P++**); single point calculations) do not significantly change the energetics (approx. ± 5 kJ/mol). All intermediates and transition

states were characterized by frequency calculation with Gaussian 03.¹⁹ The energies reported are free energies based on the SVWN/LACVP** basis set and solvent corrections with CH₃COCH₃.

References.

1. J. Benet-Buchholz, P. Comba, A. Llobet, S. Roeser, P. Vadivelu, H. Wadepohl and S. Wiesner, *Dalton Trans.*, 2009, 5910.
2. J. K. Hurst, J. L. Cape, A. E. Clark, S. Das and C. Qin, *Inorg. Chem.*, 2008, **47**, 1753.
3. N. S. Panina and M. Calligaris, *Inorg. Chim. Acta*, 2002, **334**, 165.
4. M. Kato, T. Takayanagi, T. Fujihara and A. Nagasawa, *Inorg. Chim. Acta*, 2009, **362**, 1199.
5. The modeled profile to obtain the TS1 (in Figure 5) shows a very flat potential energy surface. Due to this, TS1 for [Ru^{IV}(L²)(L³)(O)]²⁺ is hard to compute. However, TS1 is estimated to have an energy of approximately 10 kJ/mol.
6. N. Aebischer, E. Sidorenkova, M. Ravera, G. Laurenczy, D. Osella, J. Weber and A. E. Merbach, *Inorg. Chem.*, 1997, **36**, 6009.
7. D. De Vito, H. Siderenkova, F. P. Rotzinger, J. Weber and A. E. Merbach, *Inorg. Chem.*, 2000, **39**, 5547.
8. M. Stener and M. Calligaris, *J. Mol. Struct. (Theochem)*, 2000, **497**, 91.
9. Schrödinger, Schrödinger LLC, New York, NY, Editon edn., 2005.
10. A. D. Becke, *J. Chem. Phys.*, 1992, **96**, 2155.
11. A. D. Becke, *J. Chem. Phys.*, 1992, **97**, 9713.
12. S. Ghosh, K. Chaitanya, K. Bhanuprakash, M. K. Nazeeruddin, M. Grätzel and P. Y. Reddy, *Inorg. Chem.*, 2006, **45**, 7600.
13. P. Hohenberg and W. Kohn, *Phys. Rev.*, 1964, **136**, B864
14. W. Kohn and L. J. Sham, *Phys. Rev. A*, 1965, **140**, 1133.
15. S. H. Vosko, L. Wilk and M. Nusair, *Can. J. Phys.*, 1980, **58**, 1200.
16. M. T. Cancès, B. Mennucci and J. Tomasi, *J. Chem. Phys.*, 1997, **107**, 3032.
17. M. Cossi, B. Barone, B. Mennucci and J. Tomasi, *Chem. Phys. Lett.*, 1998, **286**, 253.
18. M. Cossi, G. Scalmani, N. Rega and V. Barone, *J. Chem. Phys.*, 2002, **117**, 43.
19. M. J. Frisch, G. W. Trucks, H. B. Schlegel, G. E. Scuseria, M. A. Robb, J. R. Cheeseman, J. A. Montgomery Jr., T. Vreven, K. N. Kudin, J. C. Burant, J. M. Millam, S. S. Iyengar, J. Tomasi, V. Barone, B. Mennucci, M. Cossi, G. Scalmani, N. Rega, G. A. Petersson, H. Nakatsuji, M. Hada, M. Ehara, K. Toyota, R. Fukuda, J. Hasegawa, M. Ishida, T. Nakajima, Y. Honda, O. Kitao, H. Nakai, M. Klene, X. Li, J. E. Knox, H. P. Hratchian, J. B. Cross, V. Bakken, C. Adamo, J. Jaramillo, R. Gomperts, R. E. Stratmann, O. Yazyev, A. Austin, R. Cammi, C. Pomelli, J. W. Ochterski, P. Y. Ayala, K. Morokuma, G. A. Voth, P. Salvador, J. J. Dannenberg, V. G. Zakrzewski, S. Dapprich, A. D. Daniels, M. C. Strain, O. Farkas, D. K. Malick, A. D. Rabuck, K. Raghavachari, J. B. Foresman, J. V. Ortiz, Q. Cui, A. G. Baboul, S. Clifford, J. Cioslowski, B. B. Stefanov, G. Liu, A. Liashenko, P. Piskorz, I. Komaromi, R. L. Martin, D. J. Fox, T. Keith, M. A. Al-Laham, C. Y. Peng, A. Nanayakkara, M. Challacombe, P. M. W. Gill, B. Johnson, W. Chen, M. W. Wong, C. Gonzalez and J. A. Pople, Gaussian Inc., Wallingford CT, Editon edn., 2003.

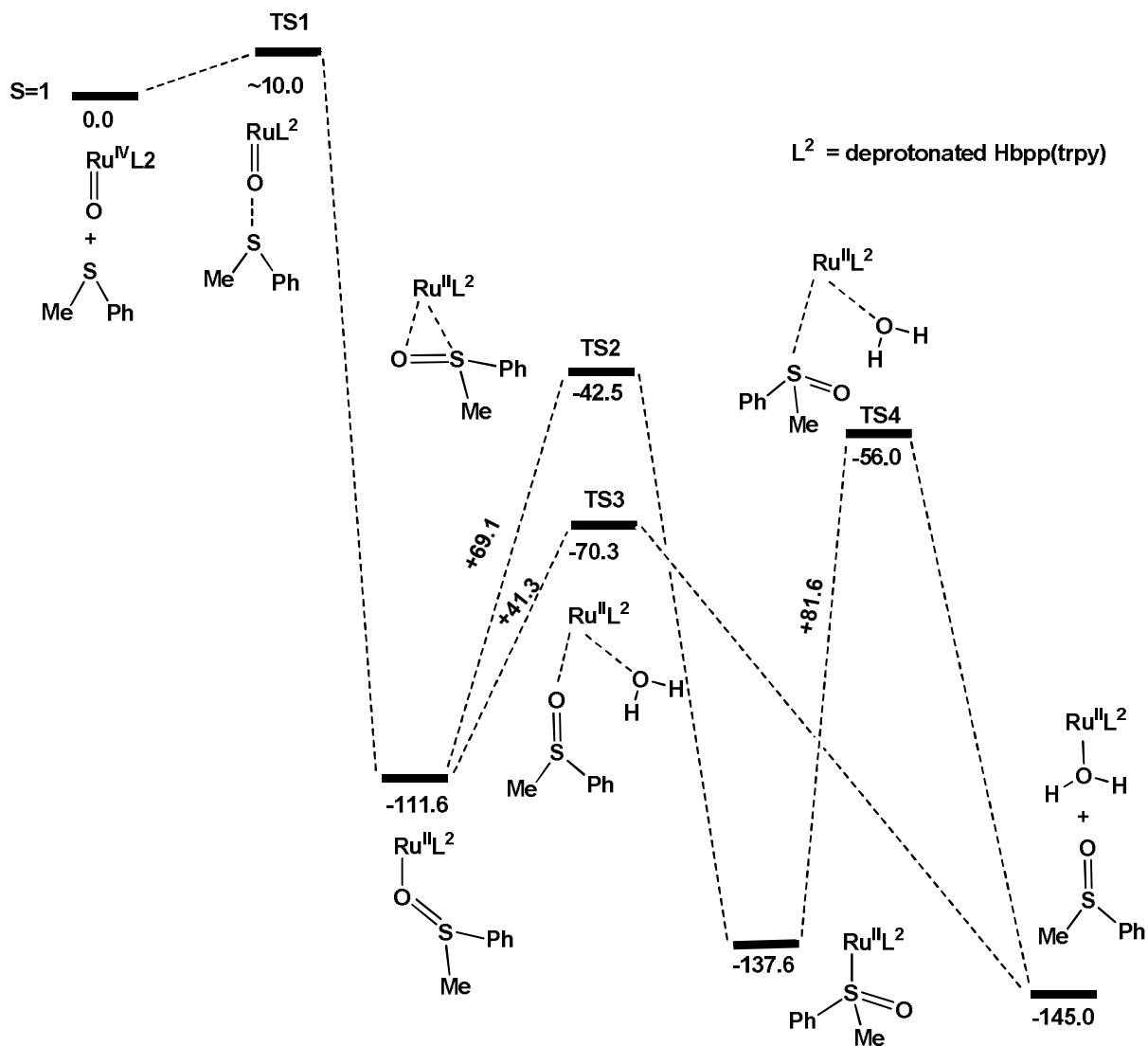


Figure S3. Computed (SVWN/lacvp**) free energy (kJ/mol) profile for the sulfoxidation of $[\text{Ru}^{\text{IV}}(\text{L}^2)(\text{L}^3)(\text{O})]^{2+}$. Solvent effect of acetone is included.

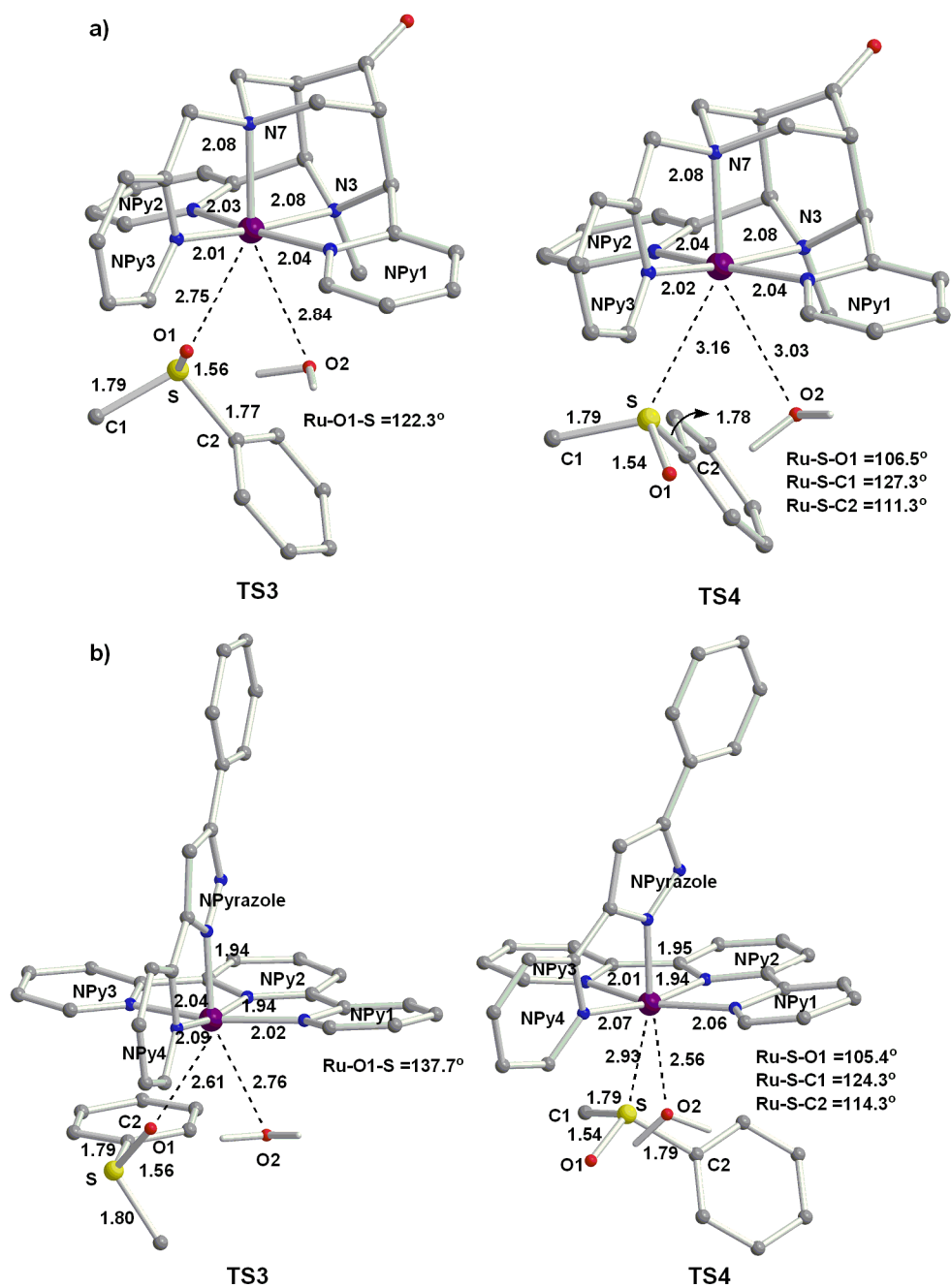
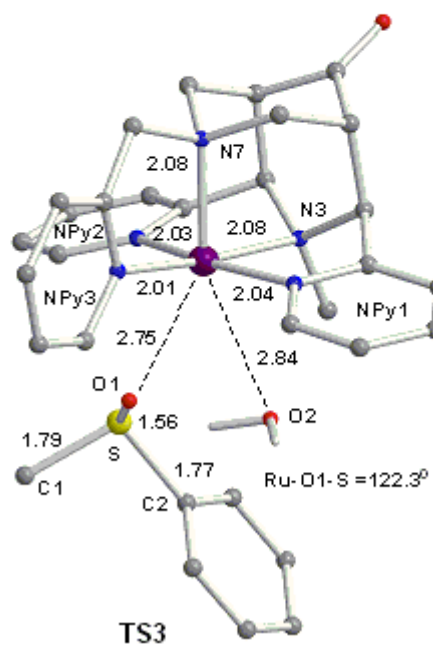
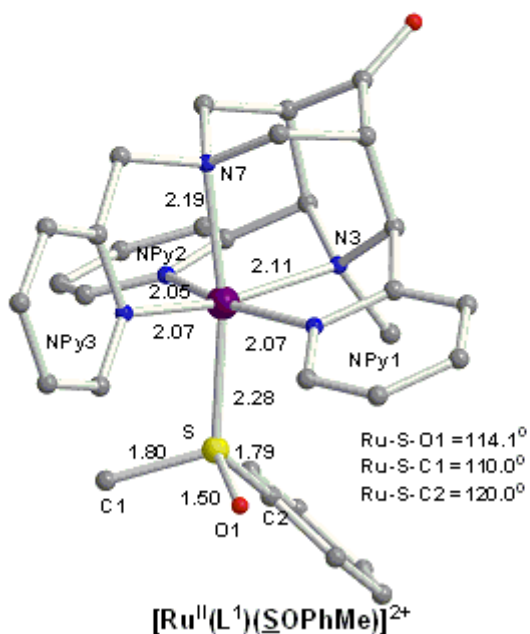
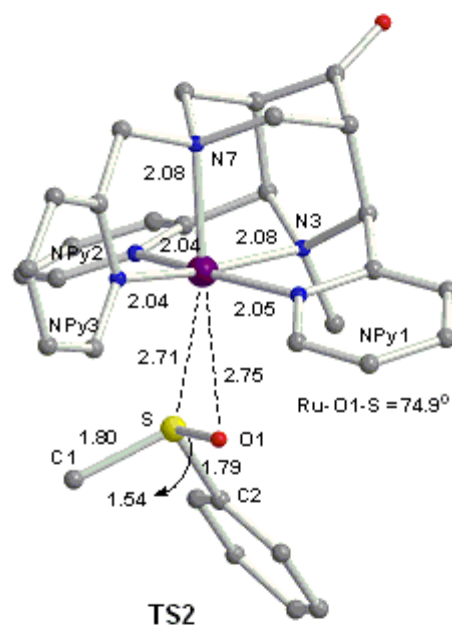
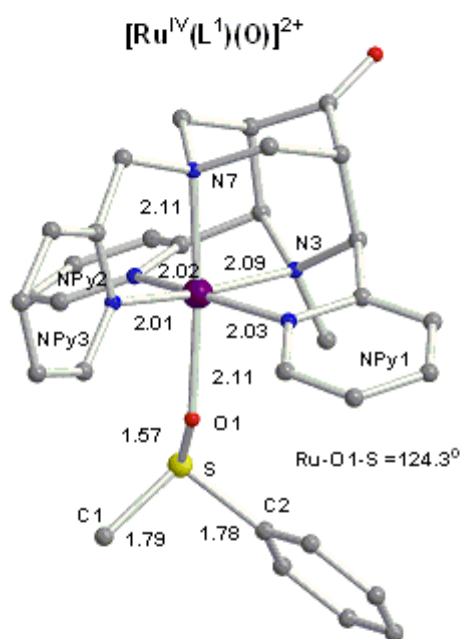
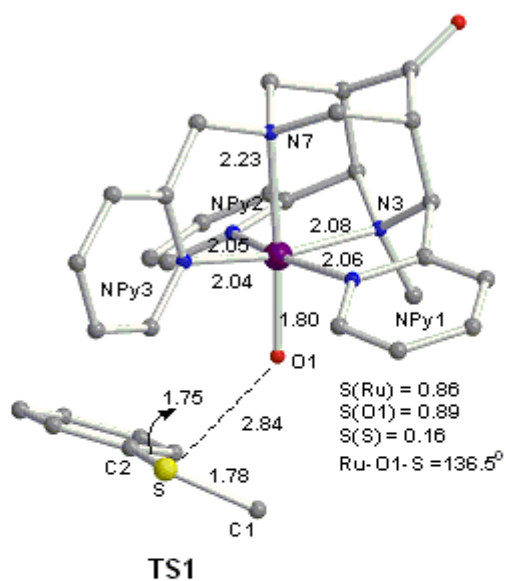
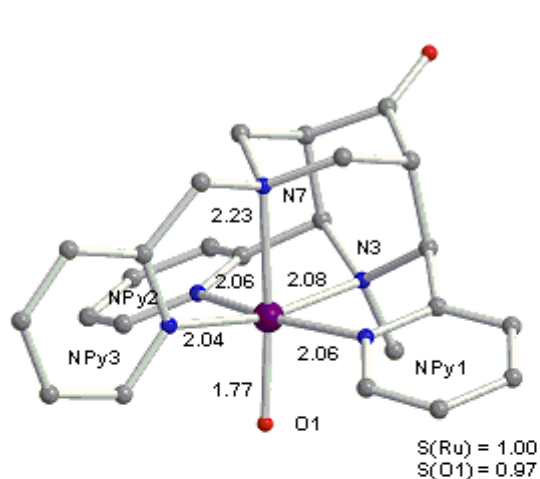


Figure S4. (a) $[\text{Ru}^{\text{IV}}(\text{L}^1)(\text{O})]^{2+}$ based TS3 and TS4 structures. (b) $[\text{Ru}^{\text{IV}}(\text{L}^2)(\text{L}^3)(\text{O})]^+$ based TS3 and TS4 structures.



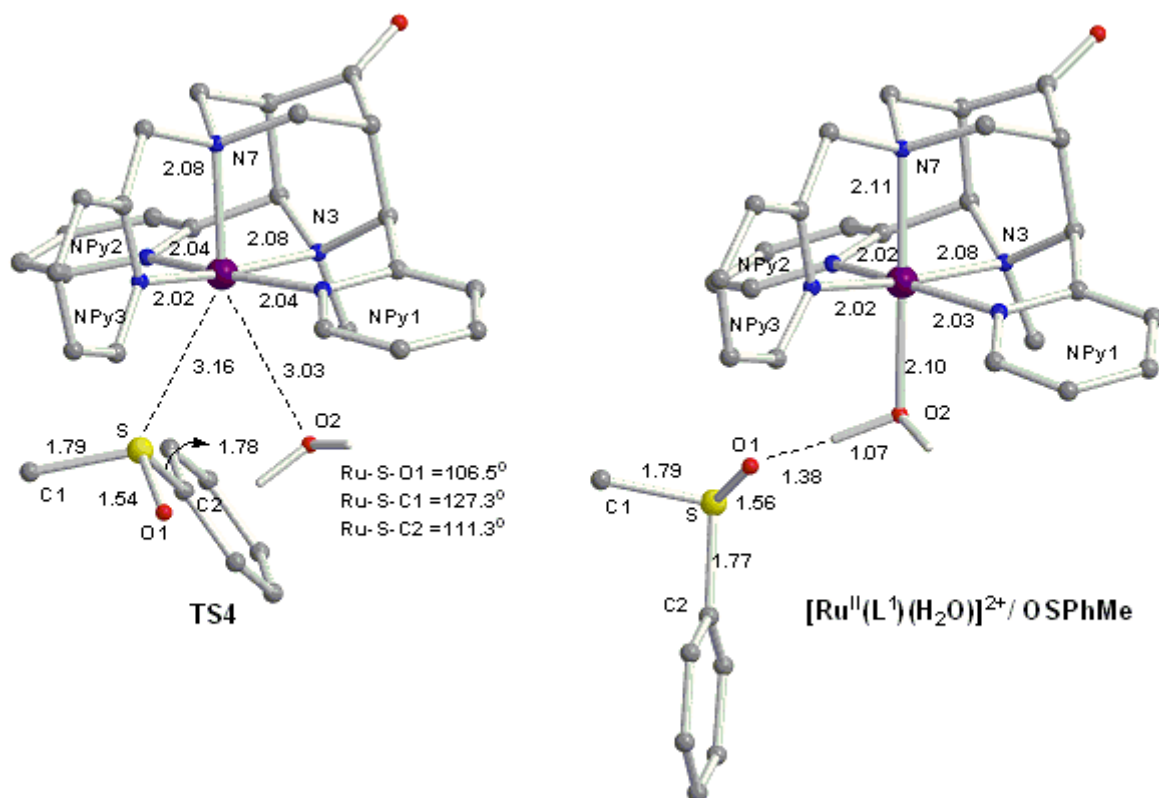
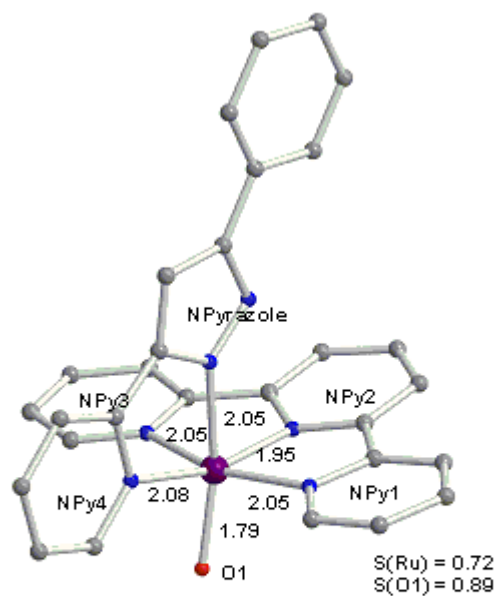
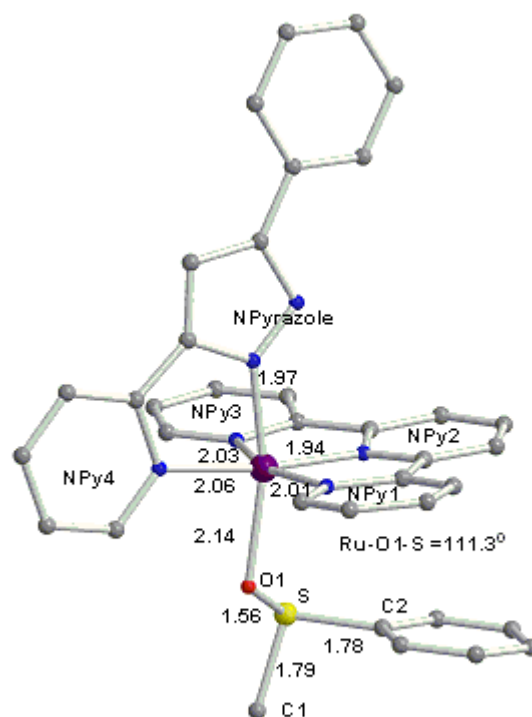


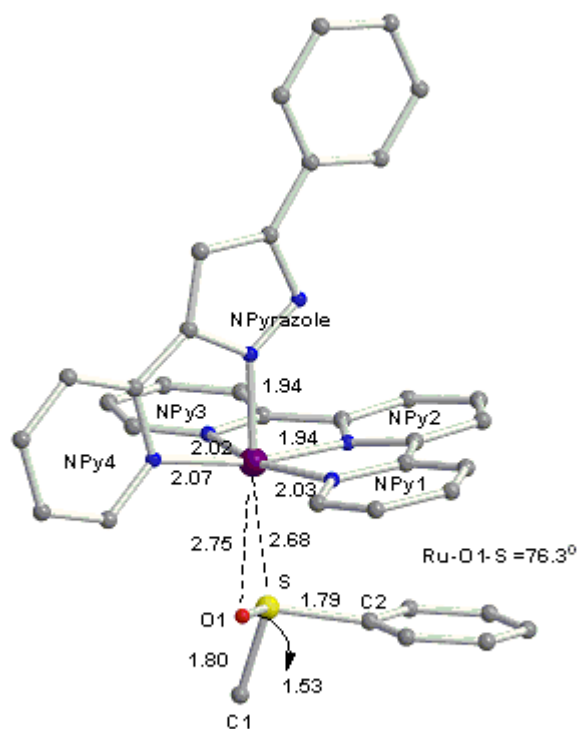
Figure S5. Computed geometries of the intermediates and transition states involved in sulfoxidation of $[\text{Ru}^{\text{IV}}(\text{L}^1)(\text{O})]^{2+}$; bond lengths in Å, valence angles in °.



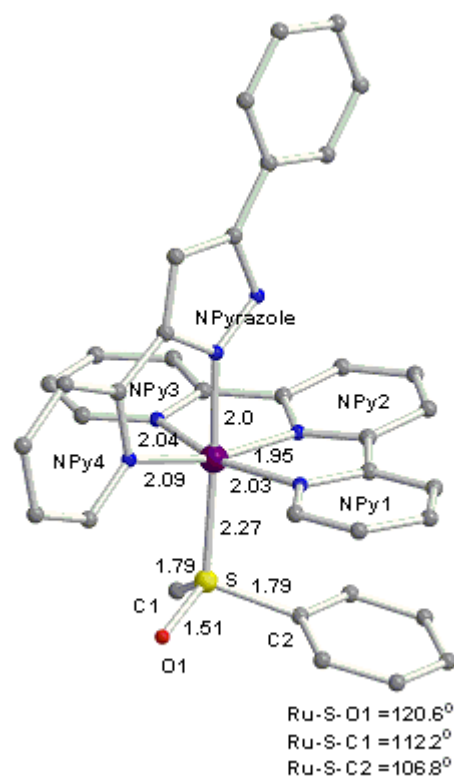
$[\text{Ru}^{\text{IV}}(\text{L}^2)(\text{L}^3)(\text{O})]^+$



$[\text{Ru}^{\text{II}}(\text{L}^2)(\text{L}^3)(\text{OSPhMe})]^+$



TS2



$[\text{Ru}^{\text{II}}(\text{L}^2)(\text{L}^3)(\text{SOPhMe})]^+$

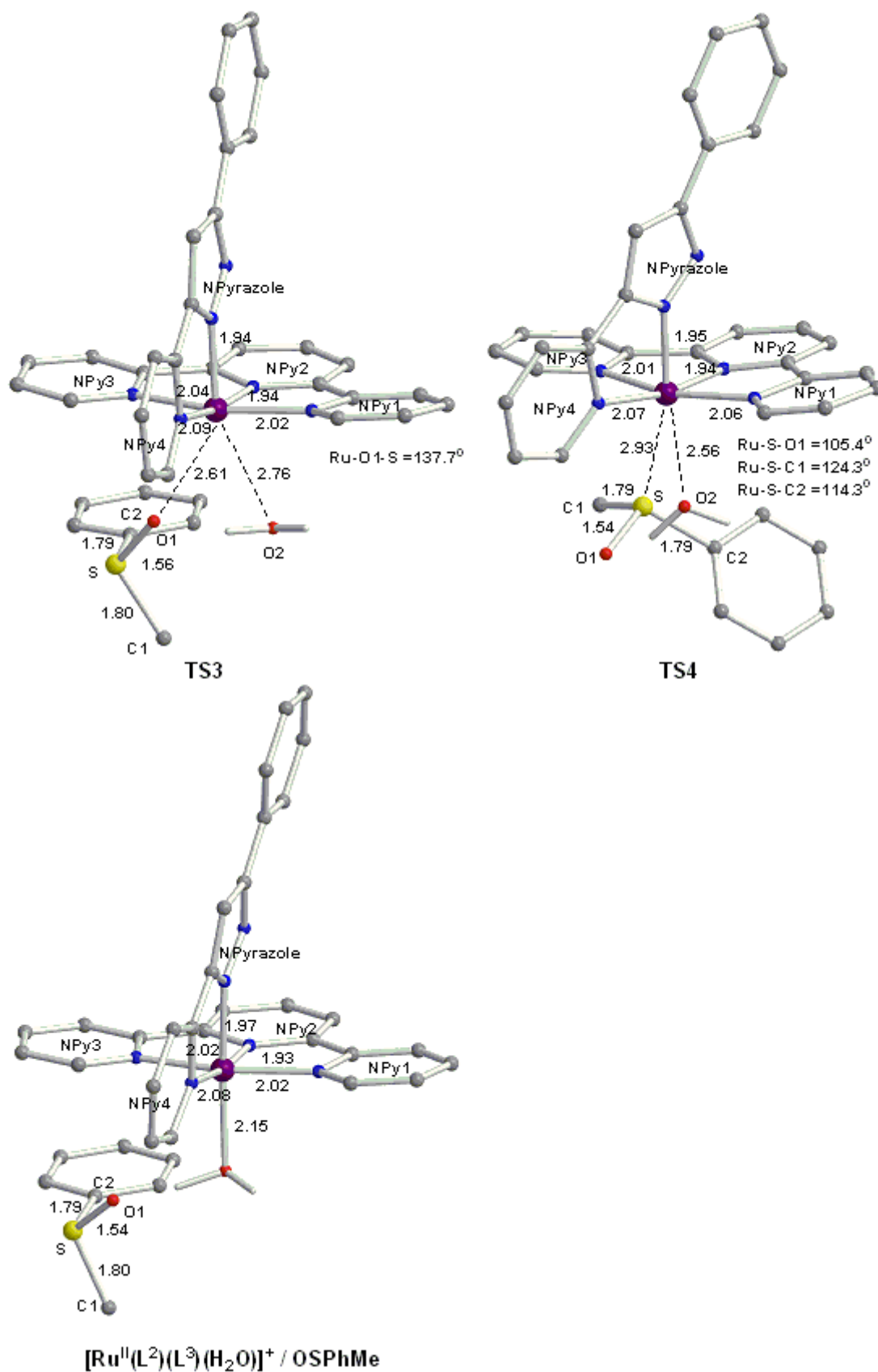


Figure S6. Computed geometries of the intermediates and transition states involved in the sulfoxidation of $[\text{Ru}^{\text{IV}}(\text{L}^2)(\text{L}^3)(\text{O})]^+$. Bond lengths in Å; Valence angles in °.

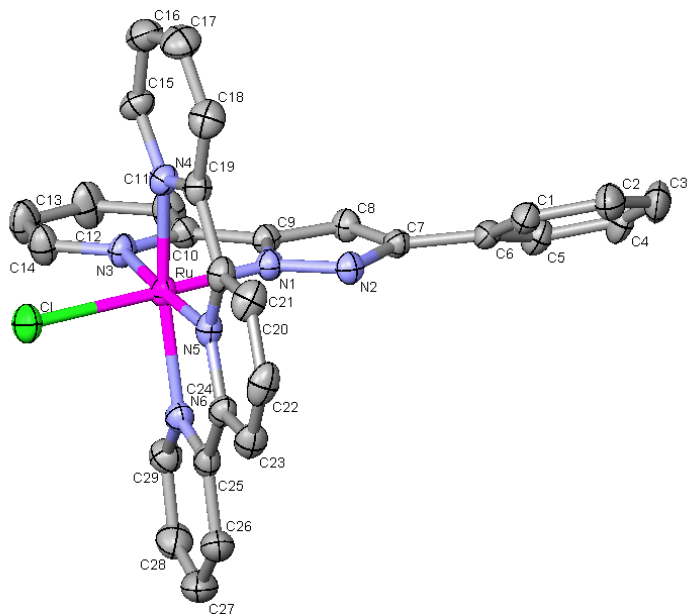


Figure S7. Atom numbering scheme for [Ru(HL²)(L³)(Cl)](PF₆)₂.

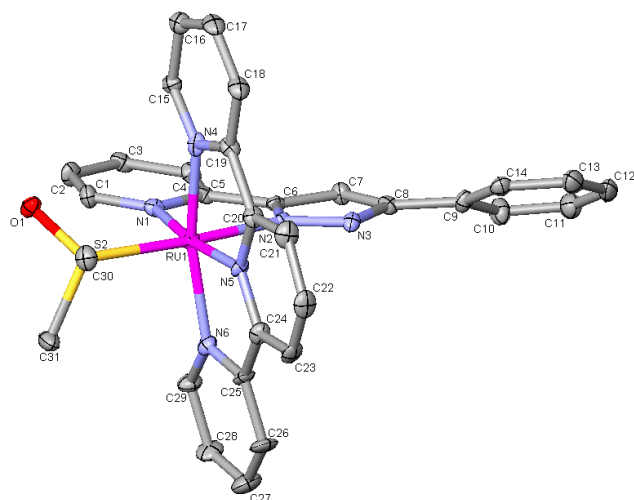


Figure S8. Atom numbering scheme for [Ru(HL²)(L³)(dmsO-S)](PF₆)₂.

Crystal data

data_exp226ap_0m

_audit_creation_method SHELXL-97
_chemical_name_systematic
;
?
;
_chemical_name_common ?
_chemical_melting_point ?
_chemical_formula_moiety ?
_chemical_formula_sum
'C34.33 H34.67 Cl0.67 F12 N6 O2.83 P2 Ru S'
_chemical_formula_weight 1023.39

loop_

_atom_type_symbol
_atom_type_description
_atom_type_scatter_dispersion_real
_atom_type_scatter_dispersion_imag
_atom_type_scatter_source
'C' 'C' 0.0033 0.0016
'International Tables Vol C Tables 4.2.6.8 and 6.1.1.4'
'H' 'H' 0.0000 0.0000
'International Tables Vol C Tables 4.2.6.8 and 6.1.1.4'
'N' 'N' 0.0061 0.0033
'International Tables Vol C Tables 4.2.6.8 and 6.1.1.4'
'O' 'O' 0.0106 0.0060
'International Tables Vol C Tables 4.2.6.8 and 6.1.1.4'
'F' 'F' 0.0171 0.0103
'International Tables Vol C Tables 4.2.6.8 and 6.1.1.4'
'P' 'P' 0.1023 0.0942
'International Tables Vol C Tables 4.2.6.8 and 6.1.1.4'
'S' 'S' 0.1246 0.1234
'International Tables Vol C Tables 4.2.6.8 and 6.1.1.4'
'Ru' 'Ru' -1.2594 0.8363
'International Tables Vol C Tables 4.2.6.8 and 6.1.1.4'

'Cl' 'Cl' 0.1484 0.1585

'International Tables Vol C Tables 4.2.6.8 and 6.1.1.4'

_symmetry_cell_setting Monoclinic
_symmetry_space_group_name_H-M P2(1)/c

loop_

_symmetry_equiv_pos_as_xyz

'x, y, z'

'-x, y+1/2, -z+1/2'

'-x, -y, -z'

'x, -y-1/2, z-1/2'

_cell_length_a 11.958(3)
_cell_length_b 11.263(3)
_cell_length_c 31.378(7)
_cell_angle_alpha 90.00
_cell_angle_beta 90.387(9)
_cell_angle_gamma 90.00
_cell_volume 4225.8(19)
_cell_formula_units_Z 4
_cell_measurement_temperature 100(2)
_cell_measurement_reflns_used 791
_cell_measurement_theta_min 2.81
_cell_measurement_theta_max 25.50

_exptl_crystal_description Plate
_exptl_crystal_colour yellow
_exptl_crystal_size_max 0.30
_exptl_crystal_size_mid 0.10
_exptl_crystal_size_min 0.02
_exptl_crystal_density_meas ?
_exptl_crystal_density_diffn 1.609
_exptl_crystal_density_method 'not measured'
_exptl_crystal_F_000 2059
_exptl_absorpt_coefficient_mu 0.633
_exptl_absorpt_correction_type empirical
_exptl_absorpt_correction_T_min 0.8434
_exptl_absorpt_correction_T_max 1.0

```
_exptl_absorpt_process_details
;
SADABS Version 2008/1 Bruker-Nonius
Blessing, Acta Cryst. (1995) A51 33-38
;
_exptl_special_details
;
It should be noted that the esd's of the cell dimensions are probably too low;
they should be multiplied by a factor of 2 to 10
;
_diffrn_ambient_temperature    100(2)
_diffrn_measurement_specimen_support
    'magnetic support whith 10 micron nylon fiber cryoloop'
_diffrn_radiation_wavelength    0.71073
_diffrn_radiation_type          MoK\alpha
_diffrn_source                  'rotating anode X-ray tube'
_diffrn_source_type             'Bruker-Nonius FR 591'
_diffrn_source_power            50
_diffrn_source_current          70
_diffrn_source_size             '3 mm x 0.3 mm fine focus'
_diffrn_radiation_monochromator 'Multilayer Montel 200 mirrors'
_diffrn_detector_type           '4K CCD area detector APEX II'
_diffrn_measurement_device_type 'Kappa 4-axis goniometer bruker-nonius'
_diffrn_measurement_method
;
Fullsphere data collection, phi and omega scans
;
_diffrn_detector_area_resol_mean 512
_diffrn_reflns_number            29121
_diffrn_reflns_av_R_equivalents 0.0726
_diffrn_reflns_av_signal/netI    0.0930
_diffrn_reflns_limit_h_min       -17
_diffrn_reflns_limit_h_max       17
_diffrn_reflns_limit_k_min       -14
_diffrn_reflns_limit_k_max       16
_diffrn_reflns_limit_l_min       -45
_diffrn_reflns_limit_l_max       44
_diffrn_reflns_theta_min         1.70
_diffrn_reflns_theta_max         30.80
```



```
_reflns_number_total      12935
_reflns_number_gt        9020
_reflns_threshold_expression  >2sigma(I)

_computing_data_collection  'Bruker APEX2 v2009.1-0'
_computing_cell_refinement  'Bruker APEX2 v2009.1-0'
_computing_data_reduction   'Bruker SAINT V7.60A'
_computing_structure_solution 'SHELXS-97 (Sheldrick, 2008)'
_computing_structure_refinement 'SHELXS-97 (Sheldrick, 2008)'
_computing_molecular_graphics 'Bruker SHELXTL'
_computing_publication_material 'Bruker SHELXTL'
```

```
_refine_special_details
```

```
;
```

Refinement of F^2 against ALL reflections. The weighted R-factor wR and goodness of fit S are based on F^2 , conventional R-factors R are based on F, with F set to zero for negative F^2 . The threshold expression of $F^2 > 2\sigma(F^2)$ is used only for calculating R-factors(gt) etc. and is not relevant to the choice of reflections for refinement. R-factors based on F^2 are statistically about twice as large as those based on F, and R-factors based on ALL data will be even larger. There a disordered dichlormethane molecule with a total occupation of 1/3 and disordered water molecules.

```
;
```

```
_refine_ls_structure_factor_coef Fsqd
_refine_ls_matrix_type      full
_refine_ls_weighting_scheme  calc
_refine_ls_weighting_details
'calc w=1/[\s^2(Fo^2)+(0.1000P)^2+0.0000P] where P=(Fo^2+2Fc^2)/3'
_atom_sites_solution_primary  direct
_atom_sites_solution_secondary difmap
_atom_sites_solution_hydrogens geom
_refine_ls_hydrogen_treatment noref
_refine_ls_extinction_method  none
_refine_ls_extinction_coef    ?
_refine_ls_number_reflns     12935
_refine_ls_number_parameters  587
_refine_ls_number_restraints  8
```

_refine_ls_R_factor_all 0.1342
_refine_ls_R_factor_gt 0.0953
_refine_ls_wR_factor_ref 0.2493
_refine_ls_wR_factor_gt 0.2331
_refine_ls_goodness_of_fit_ref 1.413
_refine_ls_restrained_S_all 1.413
_refine_ls_shift/su_max 0.001
_refine_ls_shift/su_mean 0.000

loop_

_atom_site_label
_atom_site_type_symbol

_atom_site_fract_x

_atom_site_fract_y

_atom_site_fract_z

_atom_site_U_iso_or_equiv

_atom_site_adp_type

_atom_site_occupancy

_atom_site_symmetry_multiplicity

_atom_site_calc_flag

_atom_site_refinement_flags

_atom_site_disorder_assembly

_atom_site_disorder_group

Cl1B Cl 0.7815(9) 0.5405(7) 0.4212(3) 0.086(2) Uani 0.33 1 d PD A .

Cl2B Cl 0.8979(10) 0.3300(12) 0.4529(5) 0.084(4) Uani 0.22 1 d P A 1

Cl2' Cl 0.923(2) 0.371(3) 0.4853(11) 0.16(2) Uani 0.11 1 d PD A 2

C1B C 0.8885(18) 0.477(4) 0.4492(10) 0.10(2) Uani 0.33 1 d PD . .

H1BA H 0.9591 0.5063 0.4366 0.122 Uiso 0.22 1 calc PR A 1

H1BB H 0.8855 0.5091 0.4786 0.122 Uiso 0.22 1 calc PR A 1

H1BC H 0.9219 0.5484 0.4629 0.122 Uiso 0.11 1 calc PR A 2

H1BD H 0.9405 0.4578 0.4258 0.122 Uiso 0.11 1 calc PR A 2

O1W O 0.866(5) 0.483(4) 0.4486(14) 0.18(3) Uani 0.33 1 d P B 3

O2W O 1.0000 0.5000 0.5000 0.37(11) Uani 0.17 1 d P C 3

O3W O 0.981(11) 0.540(10) 0.492(4) 0.34(5) Uani 0.33 1 d PU . 4

C1 C 0.9441(5) 0.7835(5) 0.29299(16) 0.0258(11) Uani 1 1 d . . .

H1 H 0.9194 0.8109 0.2659 0.031 Uiso 1 1 calc R . .

C2 C 1.0250(5) 0.6954(5) 0.29448(18) 0.0297(12) Uani 1 1 d . . .

H2 H 1.0534 0.6628 0.2688 0.036 Uiso 1 1 calc R . .

C3 C 1.0638(5) 0.6556(5) 0.33308(18) 0.0278(11) Uani 1 1 d . . .

H3 H 1.1200 0.5961 0.3346 0.033 Uiso 1 1 calc R . .
C4 C 1.0194(5) 0.7040(5) 0.36995(17) 0.0280(12) Uani 1 1 d . . .
H4 H 1.0437 0.6772 0.3972 0.034 Uiso 1 1 calc R . .
C5 C 0.9389(5) 0.7921(5) 0.36629(16) 0.0223(10) Uani 1 1 d . . .
C6 C 0.8936(4) 0.8531(4) 0.40320(16) 0.0208(10) Uani 1 1 d . . .
C7 C 0.9139(5) 0.8439(5) 0.44696(16) 0.0259(11) Uani 1 1 d . . .
H7 H 0.9612 0.7886 0.4611 0.031 Uiso 1 1 calc R . .
C8 C 0.8508(5) 0.9317(5) 0.46504(16) 0.0230(10) Uani 1 1 d . . .
C9 C 0.8401(5) 0.9647(5) 0.50974(16) 0.0267(11) Uani 1 1 d . . .
C10 C 0.8605(6) 0.8823(6) 0.54146(18) 0.0363(14) Uani 1 1 d . . .
H10 H 0.8790 0.8030 0.5340 0.044 Uiso 1 1 calc R . .
C11 C 0.8545(6) 0.9136(7) 0.5836(2) 0.0421(16) Uani 1 1 d . . .
H11 H 0.8689 0.8556 0.6050 0.051 Uiso 1 1 calc R . .
C12 C 0.8279(5) 1.0276(7) 0.59535(19) 0.0407(16) Uani 1 1 d . . .
H12 H 0.8254 1.0488 0.6246 0.049 Uiso 1 1 calc R . .
C13 C 0.8048(5) 1.1118(7) 0.5642(2) 0.0401(15) Uani 1 1 d . . .
H13 H 0.7841 1.1902 0.5721 0.048 Uiso 1 1 calc R . .
C14 C 0.8121(5) 1.0811(5) 0.52132(18) 0.0293(12) Uani 1 1 d . . .
H14 H 0.7980 1.1389 0.4999 0.035 Uiso 1 1 calc R . .
C15 C 0.9872(4) 1.1172(5) 0.31847(16) 0.0242(10) Uani 1 1 d . . .
H15 H 1.0239 1.0448 0.3119 0.029 Uiso 1 1 calc R . .
C16 C 1.0482(5) 1.2217(5) 0.31763(18) 0.0288(12) Uani 1 1 d . . .
H16 H 1.1257 1.2210 0.3112 0.035 Uiso 1 1 calc R . .
C17 C 0.9937(5) 1.3270(5) 0.32640(19) 0.0326(13) Uani 1 1 d . . .
H17 H 1.0331 1.4002 0.3258 0.039 Uiso 1 1 calc R . .
C18 C 0.8815(5) 1.3245(5) 0.33601(18) 0.0310(12) Uani 1 1 d . . .
H18 H 0.8434 1.3964 0.3422 0.037 Uiso 1 1 calc R . .
C19 C 0.8240(5) 1.2177(5) 0.33674(16) 0.0226(10) Uani 1 1 d . . .
C20 C 0.7043(5) 1.2060(5) 0.34585(17) 0.0247(11) Uani 1 1 d . . .
C21 C 0.6291(6) 1.2960(5) 0.3547(2) 0.0353(14) Uani 1 1 d . . .
H21 H 0.6537 1.3761 0.3556 0.042 Uiso 1 1 calc R . .
C22 C 0.5169(5) 1.2687(5) 0.3622(2) 0.0347(14) Uani 1 1 d . . .
H22 H 0.4643 1.3303 0.3671 0.042 Uiso 1 1 calc R . .
C23 C 0.4833(5) 1.1516(6) 0.36237(18) 0.0331(13) Uani 1 1 d . . .
H23 H 0.4075 1.1318 0.3678 0.040 Uiso 1 1 calc R . .
C24 C 0.5609(5) 1.0630(5) 0.35461(17) 0.0267(11) Uani 1 1 d . . .
C25 C 0.5427(5) 0.9331(5) 0.35489(18) 0.0278(11) Uani 1 1 d . . .
C26 C 0.4431(5) 0.8833(6) 0.3667(2) 0.0390(15) Uani 1 1 d . . .
H26 H 0.3817 0.9317 0.3748 0.047 Uiso 1 1 calc R . .

C27 C 0.4339(6) 0.7591(7) 0.3664(2) 0.0478(18) Uani 1 1 d . . .
H27 H 0.3663 0.7215 0.3747 0.057 Uiso 1 1 calc R . .
C28 C 0.5240(6) 0.6932(6) 0.3541(2) 0.0402(15) Uani 1 1 d . . .
H28 H 0.5187 0.6091 0.3537 0.048 Uiso 1 1 calc R . .
C29 C 0.6221(5) 0.7470(5) 0.34228(19) 0.0301(12) Uani 1 1 d . . .
H29 H 0.6836 0.6996 0.3336 0.036 Uiso 1 1 calc R . .
C30 C 0.6752(5) 1.1170(5) 0.24582(19) 0.0335(13) Uani 1 1 d . . .
H30A H 0.7234 1.1834 0.2543 0.050 Uiso 1 1 calc R . .
H30B H 0.6027 1.1243 0.2600 0.050 Uiso 1 1 calc R . .
H30C H 0.6640 1.1183 0.2149 0.050 Uiso 1 1 calc R . .
C31 C 0.6372(6) 0.8808(6) 0.24117(19) 0.0381(15) Uani 1 1 d . . .
H31A H 0.6273 0.8929 0.2104 0.057 Uiso 1 1 calc R . .
H31B H 0.5661 0.8948 0.2556 0.057 Uiso 1 1 calc R . .
H31C H 0.6619 0.7991 0.2465 0.057 Uiso 1 1 calc R . .
O1A O 0.6113(6) 0.1286(8) 0.4521(2) 0.101(3) Uani 1 1 d . . .
C1A C 0.5487(7) 0.1894(8) 0.4722(2) 0.053(2) Uani 1 1 d . . .
C2A C 0.5852(15) 0.3097(10) 0.4848(5) 0.158(8) Uani 1 1 d . . .
H2A1 H 0.6646 0.3197 0.4782 0.236 Uiso 1 1 calc R . .
H2A2 H 0.5741 0.3202 0.5155 0.236 Uiso 1 1 calc R . .
H2A3 H 0.5412 0.3689 0.4691 0.236 Uiso 1 1 calc R . .
C3A C 0.4384(11) 0.1578(15) 0.4873(6) 0.158(8) Uani 1 1 d . . .
H3A1 H 0.4381 0.0744 0.4962 0.236 Uiso 1 1 calc R . .
H3A2 H 0.3835 0.1693 0.4643 0.236 Uiso 1 1 calc R . .
H3A3 H 0.4189 0.2083 0.5116 0.236 Uiso 1 1 calc R . .
F1 F 0.2598(4) 0.0236(5) 0.30601(16) 0.0710(15) Uani 1 1 d . . .
F2 F 0.1790(5) -0.0617(7) 0.2506(2) 0.108(2) Uani 1 1 d . . .
F3 F 0.3238(6) -0.0063(5) 0.20859(18) 0.0833(18) Uani 1 1 d . . .
F4 F 0.2299(4) 0.1250(5) 0.24574(16) 0.0726(15) Uani 1 1 d . . .
F5 F 0.3595(6) -0.1120(4) 0.2695(2) 0.098(2) Uani 1 1 d . . .
F6 F 0.4052(3) 0.0777(4) 0.26618(17) 0.0618(13) Uani 1 1 d . . .
F7 F 0.3971(4) 0.4799(5) 0.42516(19) 0.0703(15) Uani 1 1 d . . .
F8 F 0.2926(5) 0.4966(5) 0.36792(16) 0.0653(14) Uani 1 1 d . . .
F9 F 0.1378(4) 0.4460(5) 0.40422(18) 0.0691(14) Uani 1 1 d . . .
F10 F 0.2452(6) 0.4253(6) 0.46318(17) 0.099(2) Uani 1 1 d . . .
F11 F 0.2904(5) 0.3263(4) 0.4049(2) 0.086(2) Uani 1 1 d . . .
F12 F 0.2435(4) 0.5953(4) 0.42630(18) 0.0637(13) Uani 1 1 d . . .
N1 N 0.8989(4) 0.8321(4) 0.32794(14) 0.0216(9) Uani 1 1 d . . .
N2 N 0.8209(3) 0.9408(4) 0.39473(13) 0.0176(8) Uani 1 1 d . . .
N3 N 0.7953(4) 0.9887(4) 0.43319(13) 0.0209(8) Uani 1 1 d . . .

H3A H 0.7489 1.0484 0.4369 0.025 Uiso 1 1 calc R . .
N4 N 0.8799(4) 1.1148(4) 0.32808(13) 0.0208(8) Uani 1 1 d . . .
N5 N 0.6663(3) 1.0926(4) 0.34521(13) 0.0203(8) Uani 1 1 d . . .
N6 N 0.6322(4) 0.8673(4) 0.34294(14) 0.0253(9) Uani 1 1 d . . .
O1 O 0.8384(3) 0.9689(4) 0.23309(12) 0.0276(8) Uani 1 1 d . . .
P1 P 0.29303(14) 0.00513(14) 0.25831(5) 0.0306(3) Uani 1 1 d . . .
P2 P 0.26734(14) 0.46022(14) 0.41536(5) 0.0339(3) Uani 1 1 d . . .
Ru1 Ru 0.77497(3) 0.96721(4) 0.331726(12) 0.01811(12) Uani 1 1 d . . .
S2 S 0.73935(10) 0.98127(11) 0.26091(4) 0.0209(3) Uani 1 1 d . . .

loop_

_atom_site_aniso_label
_atom_site_aniso_U_11
_atom_site_aniso_U_22
_atom_site_aniso_U_33
_atom_site_aniso_U_23
_atom_site_aniso_U_13
_atom_site_aniso_U_12
Cl1B 0.110(7) 0.050(4) 0.097(6) 0.001(4) -0.007(5) -0.009(4)
Cl2B 0.070(7) 0.071(7) 0.112(11) 0.046(7) 0.016(7) 0.007(6)
Cl2' 0.052(15) 0.32(7) 0.11(3) -0.06(4) 0.019(16) -0.03(3)
C1B 0.11(3) 0.15(5) 0.044(18) 0.01(2) 0.032(19) -0.08(3)
O1W 0.29(5) 0.14(3) 0.13(3) 0.02(2) 0.04(3) 0.18(4)
O2W 0.36(11) 0.35(12) 0.41(14) 0.34(12) 0.37(12) 0.34(11)
O3W 0.35(6) 0.32(7) 0.33(6) 0.03(5) 0.01(4) 0.03(5)
C1 0.031(3) 0.026(3) 0.020(2) -0.004(2) -0.002(2) 0.007(2)
C2 0.030(3) 0.029(3) 0.030(3) -0.008(2) -0.001(2) 0.013(2)
C3 0.032(3) 0.016(2) 0.035(3) -0.005(2) -0.007(2) 0.005(2)
C4 0.040(3) 0.019(2) 0.025(3) -0.001(2) -0.003(2) 0.006(2)
C5 0.028(3) 0.017(2) 0.022(2) -0.0039(19) 0.0003(19) -0.003(2)
C6 0.020(2) 0.017(2) 0.025(2) -0.0011(19) -0.0018(18) 0.0019(19)
C7 0.037(3) 0.020(2) 0.021(2) 0.002(2) -0.004(2) 0.005(2)
C8 0.029(3) 0.017(2) 0.023(2) 0.0000(19) -0.0003(19) -0.001(2)
C9 0.027(2) 0.034(3) 0.019(2) 0.001(2) 0.0028(19) 0.003(2)
C10 0.054(4) 0.030(3) 0.025(3) 0.004(2) -0.002(3) 0.001(3)
C11 0.051(4) 0.051(4) 0.025(3) 0.003(3) -0.002(3) -0.003(3)
C12 0.028(3) 0.072(5) 0.023(3) -0.012(3) 0.002(2) -0.004(3)
C13 0.034(3) 0.050(4) 0.037(3) -0.014(3) 0.003(3) 0.002(3)
C14 0.029(3) 0.031(3) 0.028(3) -0.001(2) 0.002(2) 0.004(2)

C15 0.024(2) 0.027(3) 0.022(2) 0.006(2) -0.0033(19) -0.001(2)
C16 0.030(3) 0.029(3) 0.027(3) 0.005(2) -0.003(2) -0.004(2)
C17 0.045(4) 0.022(3) 0.031(3) 0.001(2) -0.002(2) -0.010(3)
C18 0.048(4) 0.017(3) 0.028(3) 0.001(2) 0.001(2) -0.004(2)
C19 0.028(3) 0.016(2) 0.024(2) 0.0021(19) -0.0029(19) 0.002(2)
C20 0.034(3) 0.017(2) 0.023(2) 0.0013(19) -0.001(2) 0.005(2)
C21 0.044(4) 0.025(3) 0.037(3) 0.002(2) 0.002(3) 0.014(3)
C22 0.037(3) 0.029(3) 0.038(3) -0.001(2) 0.003(3) 0.018(3)
C23 0.021(3) 0.049(4) 0.030(3) 0.001(3) 0.003(2) 0.011(3)
C24 0.022(2) 0.031(3) 0.027(3) 0.002(2) 0.002(2) 0.009(2)
C25 0.021(2) 0.032(3) 0.030(3) 0.004(2) 0.005(2) -0.003(2)
C26 0.021(3) 0.043(4) 0.053(4) 0.000(3) 0.010(3) -0.008(3)
C27 0.031(3) 0.051(4) 0.062(5) 0.007(4) 0.013(3) -0.010(3)
C28 0.044(4) 0.027(3) 0.050(4) 0.008(3) 0.009(3) -0.014(3)
C29 0.030(3) 0.022(3) 0.038(3) 0.004(2) 0.005(2) -0.003(2)
C30 0.041(3) 0.032(3) 0.027(3) 0.003(2) -0.003(2) 0.008(3)
C31 0.046(4) 0.039(3) 0.029(3) 0.000(3) -0.004(3) -0.018(3)
O1A 0.098(5) 0.156(8) 0.049(4) -0.019(4) -0.015(3) 0.095(6)
C1A 0.056(5) 0.060(5) 0.044(4) 0.000(4) 0.000(3) 0.020(4)
C2A 0.220(18) 0.042(6) 0.209(17) -0.027(8) -0.126(14) 0.018(9)
C3A 0.064(8) 0.128(13) 0.28(2) 0.067(14) 0.037(11) -0.011(9)
F1 0.067(3) 0.102(4) 0.044(3) 0.013(3) 0.009(2) 0.017(3)
F2 0.085(4) 0.146(6) 0.092(5) 0.002(4) -0.020(3) -0.078(4)
F3 0.107(5) 0.085(4) 0.058(3) -0.023(3) 0.024(3) -0.015(3)
F4 0.063(3) 0.081(4) 0.074(3) 0.028(3) 0.006(3) 0.034(3)
F5 0.118(5) 0.025(2) 0.150(6) 0.012(3) 0.050(4) 0.020(3)
F6 0.030(2) 0.052(3) 0.104(4) -0.004(3) -0.009(2) -0.011(2)
F7 0.041(2) 0.082(4) 0.088(4) -0.009(3) -0.018(2) 0.018(3)
F8 0.074(3) 0.075(3) 0.047(3) 0.015(2) 0.006(2) 0.007(3)
F9 0.037(2) 0.078(4) 0.092(4) -0.017(3) 0.007(2) -0.010(2)
F10 0.133(5) 0.106(5) 0.057(3) 0.040(3) 0.032(3) 0.055(4)
F11 0.088(4) 0.023(2) 0.148(5) -0.001(3) 0.057(4) 0.004(2)
F12 0.052(3) 0.033(2) 0.107(4) -0.009(2) 0.008(3) 0.011(2)
N1 0.026(2) 0.017(2) 0.022(2) 0.0006(16) -0.0016(16) -0.0006(18)
N2 0.0195(19) 0.0151(19) 0.0184(18) 0.0010(15) 0.0015(14) 0.0026(16)
N3 0.028(2) 0.0153(19) 0.0191(19) 0.0005(15) 0.0029(16) 0.0022(17)
N4 0.022(2) 0.024(2) 0.0168(18) 0.0055(16) -0.0007(15) 0.0032(18)
N5 0.0167(19) 0.019(2) 0.026(2) 0.0015(16) 0.0041(16) 0.0040(16)
N6 0.028(2) 0.025(2) 0.023(2) 0.0044(18) 0.0019(17) 0.0008(19)

O1 0.0258(18) 0.036(2) 0.0215(17) 0.0054(16) 0.0043(14) 0.0043(18)
P1 0.0318(8) 0.0219(7) 0.0381(8) -0.0051(6) 0.0001(6) -0.0044(6)
P2 0.0368(8) 0.0250(7) 0.0399(8) 0.0030(6) 0.0035(6) 0.0082(7)
Ru1 0.01819(19) 0.0167(2) 0.01948(19) 0.00191(15) 0.00153(12) 0.00226(16)
S2 0.0194(5) 0.0229(6) 0.0204(5) 0.0014(5) -0.0010(4) 0.0006(5)

_geom_special_details

;

All esds (except the esd in the dihedral angle between two l.s. planes) are estimated using the full covariance matrix. The cell esds are taken into account individually in the estimation of esds in distances, angles and torsion angles; correlations between esds in cell parameters are only used when they are defined by crystal symmetry. An approximate (isotropic) treatment of cell esds is used for estimating esds involving l.s. planes.

;

loop_

_geom_bond_atom_site_label_1

_geom_bond_atom_site_label_2

_geom_bond_distance

_geom_bond_site_symmetry_2

_geom_bond_publ_flag

C11B C1B 1.701(10) . ?

C12B C1B 1.67(4) . ?

C12' C1B 1.703(10) . ?

C1B O3W 1.87(16) . ?

O3W O3W 1.12(17) 3_766 ?

C1 N1 1.343(7) . ?

C1 C2 1.386(7) . ?

C2 C3 1.370(8) . ?

C3 C4 1.388(8) . ?

C4 C5 1.387(7) . ?

C5 N1 1.368(7) . ?

C5 C6 1.454(7) . ?

C6 N2 1.341(6) . ?

C6 C7 1.397(7) . ?

C7 C8 1.369(7) . ?

C8 N3 1.357(7) . ?

C8 C9 1.458(7) . ?

C9 C10 1.381(8) . ?
C9 C14 1.401(8) . ?
C10 C11 1.371(8) . ?
C11 C12 1.374(10) . ?
C12 C13 1.388(10) . ?
C13 C14 1.393(8) . ?
C15 N4 1.321(6) . ?
C15 C16 1.384(8) . ?
C16 C17 1.382(8) . ?
C17 C18 1.377(9) . ?
C18 C19 1.386(7) . ?
C19 N4 1.366(7) . ?
C19 C20 1.467(8) . ?
C20 N5 1.357(7) . ?
C20 C21 1.384(8) . ?
C21 C22 1.398(9) . ?
C22 C23 1.379(9) . ?
C23 C24 1.385(8) . ?
C24 N5 1.338(7) . ?
C24 C25 1.480(8) . ?
C25 N6 1.357(7) . ?
C25 C26 1.370(8) . ?
C26 C27 1.403(10) . ?
C27 C28 1.367(10) . ?
C28 C29 1.373(8) . ?
C29 N6 1.360(7) . ?
C30 S2 1.773(6) . ?
C31 S2 1.774(6) . ?
O1A C1A 1.196(9) . ?
C1A C3A 1.450(14) . ?
C1A C2A 1.476(14) . ?
F1 P1 1.565(5) . ?
F2 P1 1.574(5) . ?
F3 P1 1.610(6) . ?
F4 P1 1.595(5) . ?
F5 P1 1.578(5) . ?
F6 P1 1.589(4) . ?
F7 P2 1.595(5) . ?
F8 P2 1.575(5) . ?

F9 P2 1.593(5) . ?
F10 P2 1.575(5) . ?
F11 P2 1.569(5) . ?
F12 P2 1.586(5) . ?
N1 Ru1 2.128(4) . ?
N2 N3 1.358(6) . ?
N2 Ru1 2.070(4) . ?
N4 Ru1 2.086(4) . ?
N5 Ru1 1.967(4) . ?
N6 Ru1 2.077(5) . ?
O1 S2 1.482(4) . ?
Ru1 S2 2.2653(14) . ?

loop_

_geom_angle_atom_site_label_1
_geom_angle_atom_site_label_2
_geom_angle_atom_site_label_3
_geom_angle
_geom_angle_site_symmetry_1
_geom_angle_site_symmetry_3
_geom_angle_publ_flag
Cl2B C1B Cl1B 120(2) . . ?
Cl2B C1B Cl2' 40.1(15) . . ?
Cl1B C1B Cl2' 145(2) . . ?
Cl2B C1B O3W 107(3) . . ?
Cl1B C1B O3W 131(4) . . ?
Cl2' C1B O3W 69(3) . . ?
O3W O3W C1B 105(10) 3_766 . ?
N1 C1 C2 123.3(5) . . ?
C3 C2 C1 119.8(5) . . ?
C2 C3 C4 118.6(5) . . ?
C5 C4 C3 118.8(5) . . ?
N1 C5 C4 123.1(5) . . ?
N1 C5 C6 114.5(5) . . ?
C4 C5 C6 122.3(5) . . ?
N2 C6 C7 111.0(4) . . ?
N2 C6 C5 115.8(4) . . ?
C7 C6 C5 133.2(5) . . ?
C8 C7 C6 105.1(5) . . ?

N3 C8 C7 107.7(4) . . ?
N3 C8 C9 122.8(5) . . ?
C7 C8 C9 129.4(5) . . ?
C10 C9 C14 118.9(5) . . ?
C10 C9 C8 120.4(5) . . ?
C14 C9 C8 120.7(5) . . ?
C11 C10 C9 120.8(6) . . ?
C10 C11 C12 120.8(6) . . ?
C11 C12 C13 119.7(6) . . ?
C12 C13 C14 119.8(6) . . ?
C13 C14 C9 120.0(6) . . ?
N4 C15 C16 122.3(5) . . ?
C17 C16 C15 118.5(6) . . ?
C18 C17 C16 119.2(5) . . ?
C17 C18 C19 120.4(5) . . ?
N4 C19 C18 119.3(5) . . ?
N4 C19 C20 116.2(5) . . ?
C18 C19 C20 124.5(5) . . ?
N5 C20 C21 118.3(5) . . ?
N5 C20 C19 114.1(4) . . ?
C21 C20 C19 127.6(5) . . ?
C20 C21 C22 119.9(6) . . ?
C23 C22 C21 119.4(5) . . ?
C22 C23 C24 119.5(6) . . ?
N5 C24 C23 119.5(6) . . ?
N5 C24 C25 112.7(5) . . ?
C23 C24 C25 127.8(5) . . ?
N6 C25 C26 122.7(6) . . ?
N6 C25 C24 115.0(5) . . ?
C26 C25 C24 122.3(5) . . ?
C25 C26 C27 118.3(6) . . ?
C28 C27 C26 118.7(6) . . ?
C27 C28 C29 120.9(6) . . ?
N6 C29 C28 120.7(6) . . ?
O1A C1A C3A 127.2(12) . . ?
O1A C1A C2A 118.8(12) . . ?
C3A C1A C2A 113.9(12) . . ?
C1 N1 C5 116.4(5) . . ?
C1 N1 Ru1 128.4(4) . . ?

C5 N1 Ru1 115.2(3) . . ?
C6 N2 N3 105.4(4) . . ?
C6 N2 Ru1 117.5(3) . . ?
N3 N2 Ru1 137.0(3) . . ?
C8 N3 N2 110.7(4) . . ?
C15 N4 C19 120.4(5) . . ?
C15 N4 Ru1 127.9(4) . . ?
C19 N4 Ru1 111.7(3) . . ?
C24 N5 C20 123.2(5) . . ?
C24 N5 Ru1 119.6(4) . . ?
C20 N5 Ru1 117.2(4) . . ?
C25 N6 C29 118.6(5) . . ?
C25 N6 Ru1 113.7(4) . . ?
C29 N6 Ru1 127.6(4) . . ?
F1 P1 F2 89.1(3) . . ?
F1 P1 F5 91.7(3) . . ?
F2 P1 F5 94.0(4) . . ?
F1 P1 F6 90.1(3) . . ?
F2 P1 F6 177.6(4) . . ?
F5 P1 F6 88.4(3) . . ?
F1 P1 F4 90.1(3) . . ?
F2 P1 F4 87.6(4) . . ?
F5 P1 F4 177.6(3) . . ?
F6 P1 F4 90.0(3) . . ?
F1 P1 F3 176.6(3) . . ?
F2 P1 F3 91.0(4) . . ?
F5 P1 F3 91.7(3) . . ?
F6 P1 F3 89.6(3) . . ?
F4 P1 F3 86.5(3) . . ?
F11 P2 F8 91.0(3) . . ?
F11 P2 F10 89.5(3) . . ?
F8 P2 F10 178.4(4) . . ?
F11 P2 F12 179.5(3) . . ?
F8 P2 F12 89.5(3) . . ?
F10 P2 F12 90.1(3) . . ?
F11 P2 F9 91.7(3) . . ?
F8 P2 F9 90.6(3) . . ?
F10 P2 F9 90.8(4) . . ?
F12 P2 F9 88.2(3) . . ?

F11 P2 F7 90.1(3) . . ?
F8 P2 F7 87.3(3) . . ?
F10 P2 F7 91.2(4) . . ?
F12 P2 F7 90.1(3) . . ?
F9 P2 F7 177.3(3) . . ?
N5 Ru1 N2 93.96(17) . . ?
N5 Ru1 N6 78.91(19) . . ?
N2 Ru1 N6 88.48(17) . . ?
N5 Ru1 N4 80.70(18) . . ?
N2 Ru1 N4 90.62(16) . . ?
N6 Ru1 N4 159.47(18) . . ?
N5 Ru1 N1 170.65(17) . . ?
N2 Ru1 N1 76.72(16) . . ?
N6 Ru1 N1 101.25(18) . . ?
N4 Ru1 N1 98.50(17) . . ?
N5 Ru1 S2 92.33(13) . . ?
N2 Ru1 S2 173.69(12) . . ?
N6 Ru1 S2 93.14(13) . . ?
N4 Ru1 S2 89.98(11) . . ?
N1 Ru1 S2 96.99(12) . . ?
O1 S2 C30 105.6(3) . . ?
O1 S2 C31 106.6(3) . . ?
C30 S2 C31 99.3(3) . . ?
O1 S2 Ru1 115.18(16) . . ?
C30 S2 Ru1 113.6(2) . . ?
C31 S2 Ru1 115.0(2) . . ?

loop_

_geom_torsion_atom_site_label_1
_geom_torsion_atom_site_label_2
_geom_torsion_atom_site_label_3
_geom_torsion_atom_site_label_4
_geom_torsion
_geom_torsion_site_symmetry_1
_geom_torsion_site_symmetry_2
_geom_torsion_site_symmetry_3
_geom_torsion_site_symmetry_4
_geom_torsion_publ_flag
Cl2B C1B O3W O3W 2(15) . . . 3_766 ?

C11B C1B O3W O3W 163(11) . . . 3_766 ?
C12' C1B O3W O3W 17(13) . . . 3_766 ?
N1 C1 C2 C3 -1.2(9) . . . ?
C1 C2 C3 C4 0.9(9) . . . ?
C2 C3 C4 C5 -1.1(9) . . . ?
C3 C4 C5 N1 1.6(8) . . . ?
C3 C4 C5 C6 -175.7(5) . . . ?
N1 C5 C6 N2 -1.1(7) . . . ?
C4 C5 C6 N2 176.5(5) . . . ?
N1 C5 C6 C7 -177.4(5) . . . ?
C4 C5 C6 C7 0.2(9) . . . ?
N2 C6 C7 C8 -0.8(6) . . . ?
C5 C6 C7 C8 175.7(6) . . . ?
C6 C7 C8 N3 0.7(6) . . . ?
C6 C7 C8 C9 -179.2(6) . . . ?
N3 C8 C9 C10 155.0(6) . . . ?
C7 C8 C9 C10 -25.1(9) . . . ?
N3 C8 C9 C14 -26.8(8) . . . ?
C7 C8 C9 C14 153.1(6) . . . ?
C14 C9 C10 C11 -0.5(10) . . . ?
C8 C9 C10 C11 177.7(6) . . . ?
C9 C10 C11 C12 0.0(11) . . . ?
C10 C11 C12 C13 1.2(10) . . . ?
C11 C12 C13 C14 -2.0(10) . . . ?
C12 C13 C14 C9 1.5(9) . . . ?
C10 C9 C14 C13 -0.2(9) . . . ?
C8 C9 C14 C13 -178.5(5) . . . ?
N4 C15 C16 C17 -1.3(8) . . . ?
C15 C16 C17 C18 0.6(8) . . . ?
C16 C17 C18 C19 -0.2(8) . . . ?
C17 C18 C19 N4 0.4(8) . . . ?
C17 C18 C19 C20 -178.9(5) . . . ?
N4 C19 C20 N5 1.3(7) . . . ?
C18 C19 C20 N5 -179.4(5) . . . ?
N4 C19 C20 C21 -178.7(5) . . . ?
C18 C19 C20 C21 0.6(9) . . . ?
N5 C20 C21 C22 -0.7(8) . . . ?
C19 C20 C21 C22 179.3(6) . . . ?
C20 C21 C22 C23 2.5(9) . . . ?

C21 C22 C23 C24 -0.7(9) ?
C22 C23 C24 N5 -2.9(8) ?
C22 C23 C24 C25 177.7(5) ?
N5 C24 C25 N6 -4.2(7) ?
C23 C24 C25 N6 175.2(5) ?
N5 C24 C25 C26 175.3(6) ?
C23 C24 C25 C26 -5.3(9) ?
N6 C25 C26 C27 0.2(10) ?
C24 C25 C26 C27 -179.3(6) ?
C25 C26 C27 C28 -0.7(11) ?
C26 C27 C28 C29 0.3(11) ?
C27 C28 C29 N6 0.6(10) ?
C2 C1 N1 C5 1.6(8) ?
C2 C1 N1 Ru1 179.9(4) ?
C4 C5 N1 C1 -1.8(8) ?
C6 C5 N1 C1 175.7(5) ?
C4 C5 N1 Ru1 179.6(4) ?
C6 C5 N1 Ru1 -2.8(6) ?
C7 C6 N2 N3 0.5(6) ?
C5 C6 N2 N3 -176.6(4) ?
C7 C6 N2 Ru1 -178.2(3) ?
C5 C6 N2 Ru1 4.7(6) ?
C7 C8 N3 N2 -0.4(6) ?
C9 C8 N3 N2 179.5(5) ?
C6 N2 N3 C8 -0.1(5) ?
Ru1 N2 N3 C8 178.3(4) ?
C16 C15 N4 C19 1.5(7) ?
C16 C15 N4 Ru1 -179.2(4) ?
C18 C19 N4 C15 -1.0(7) ?
C20 C19 N4 C15 178.3(4) ?
C18 C19 N4 Ru1 179.5(4) ?
C20 C19 N4 Ru1 -1.1(5) ?
C23 C24 N5 C20 5.0(8) ?
C25 C24 N5 C20 -175.5(5) ?
C23 C24 N5 Ru1 -177.3(4) ?
C25 C24 N5 Ru1 2.1(6) ?
C21 C20 N5 C24 -3.2(8) ?
C19 C20 N5 C24 176.9(5) ?
C21 C20 N5 Ru1 179.1(4) ?

C19 C20 N5 Ru1 -0.8(6) ?
C26 C25 N6 C29 0.6(8) ?
C24 C25 N6 C29 -179.9(5) ?
C26 C25 N6 Ru1 -175.3(5) ?
C24 C25 N6 Ru1 4.3(6) ?
C28 C29 N6 C25 -1.0(8) ?
C28 C29 N6 Ru1 174.2(5) ?
C24 N5 Ru1 N2 -87.6(4) ?
C20 N5 Ru1 N2 90.2(4) ?
C24 N5 Ru1 N6 0.1(4) ?
C20 N5 Ru1 N6 177.8(4) ?
C24 N5 Ru1 N4 -177.6(4) ?
C20 N5 Ru1 N4 0.2(4) ?
C24 N5 Ru1 N1 -91.8(11) ?
C20 N5 Ru1 N1 86.0(11) ?
C24 N5 Ru1 S2 92.8(4) ?
C20 N5 Ru1 S2 -89.4(4) ?
C6 N2 Ru1 N5 176.0(4) ?
N3 N2 Ru1 N5 -2.2(5) ?
C6 N2 Ru1 N6 97.2(4) ?
N3 N2 Ru1 N6 -81.0(5) ?
C6 N2 Ru1 N4 -103.3(4) ?
N3 N2 Ru1 N4 78.5(5) ?
C6 N2 Ru1 N1 -4.7(4) ?
N3 N2 Ru1 N1 177.1(5) ?
C6 N2 Ru1 S2 -7.8(14) ?
N3 N2 Ru1 S2 174.0(8) ?
C25 N6 Ru1 N5 -2.5(4) ?
C29 N6 Ru1 N5 -177.9(5) ?
C25 N6 Ru1 N2 91.9(4) ?
C29 N6 Ru1 N2 -83.5(5) ?
C25 N6 Ru1 N4 4.1(7) ?
C29 N6 Ru1 N4 -171.3(5) ?
C25 N6 Ru1 N1 168.0(4) ?
C29 N6 Ru1 N1 -7.4(5) ?
C25 N6 Ru1 S2 -94.2(4) ?
C29 N6 Ru1 S2 90.4(5) ?
C15 N4 Ru1 N5 -178.8(4) ?
C19 N4 Ru1 N5 0.5(3) ?

C15 N4 Ru1 N2 87.3(4) ?
C19 N4 Ru1 N2 -93.4(3) ?
C15 N4 Ru1 N6 174.6(4) ?
C19 N4 Ru1 N6 -6.1(7) ?
C15 N4 Ru1 N1 10.6(4) ?
C19 N4 Ru1 N1 -170.0(3) ?
C15 N4 Ru1 S2 -86.5(4) ?
C19 N4 Ru1 S2 92.9(3) ?
C1 N1 Ru1 N5 -170.1(9) ?
C5 N1 Ru1 N5 8.3(13) ?
C1 N1 Ru1 N2 -174.4(5) ?
C5 N1 Ru1 N2 4.0(4) ?
C1 N1 Ru1 N6 99.9(5) ?
C5 N1 Ru1 N6 -81.8(4) ?
C1 N1 Ru1 N4 -85.7(5) ?
C5 N1 Ru1 N4 92.6(4) ?
C1 N1 Ru1 S2 5.3(5) ?
C5 N1 Ru1 S2 -176.4(3) ?
N5 Ru1 S2 O1 141.6(2) ?
N2 Ru1 S2 O1 -34.6(11) ?
N6 Ru1 S2 O1 -139.4(2) ?
N4 Ru1 S2 O1 60.9(2) ?
N1 Ru1 S2 O1 -37.7(2) ?
N5 Ru1 S2 C30 19.5(3) ?
N2 Ru1 S2 C30 -156.7(11) ?
N6 Ru1 S2 C30 98.5(3) ?
N4 Ru1 S2 C30 -61.2(3) ?
N1 Ru1 S2 C30 -159.7(3) ?
N5 Ru1 S2 C31 -93.9(3) ?
N2 Ru1 S2 C31 89.9(11) ?
N6 Ru1 S2 C31 -14.9(3) ?
N4 Ru1 S2 C31 -174.6(3) ?
N1 Ru1 S2 C31 86.9(3) ?

_diffn_measured_fraction_theta_max 0.977
_diffn_reflns_theta_full 30.80
_diffn_measured_fraction_theta_full 0.977
_refine_diff_density_max 3.812
_refine_diff_density_min -3.477

_refine_diff_density_rms 0.192